

Roh, Kosan; Chung, Wonsuk; Lee, Hyejin; Park, Seungman; Lee, Jay H.

Article

Impacts of deploying co-electrolysis of CO₂ and H₂O in the power generation sector: A case study for South Korea

Energy Reports

Provided in Cooperation with:

Elsevier

Suggested Citation: Roh, Kosan; Chung, Wonsuk; Lee, Hyejin; Park, Seungman; Lee, Jay H. (2020) : Impacts of deploying co-electrolysis of CO₂ and H₂O in the power generation sector: A case study for South Korea, Energy Reports, ISSN 2352-4847, Elsevier, Amsterdam, Vol. 6, pp. 761-770,
<https://doi.org/10.1016/j.egy.2020.03.034>

This Version is available at:

<https://hdl.handle.net/10419/244074>

Standard-Nutzungsbedingungen:

Die Dokumente auf EconStor dürfen zu eigenen wissenschaftlichen Zwecken und zum Privatgebrauch gespeichert und kopiert werden.

Sie dürfen die Dokumente nicht für öffentliche oder kommerzielle Zwecke vervielfältigen, öffentlich ausstellen, öffentlich zugänglich machen, vertreiben oder anderweitig nutzen.

Sofern die Verfasser die Dokumente unter Open-Content-Lizenzen (insbesondere CC-Lizenzen) zur Verfügung gestellt haben sollten, gelten abweichend von diesen Nutzungsbedingungen die in der dort genannten Lizenz gewährten Nutzungsrechte.

Terms of use:

Documents in EconStor may be saved and copied for your personal and scholarly purposes.

You are not to copy documents for public or commercial purposes, to exhibit the documents publicly, to make them publicly available on the internet, or to distribute or otherwise use the documents in public.

If the documents have been made available under an Open Content Licence (especially Creative Commons Licences), you may exercise further usage rights as specified in the indicated licence.



<https://creativecommons.org/licenses/by-nc-nd/4.0/>



Research paper

Impacts of deploying co-electrolysis of CO₂ and H₂O in the power generation sector: A case study for South KoreaKosan Roh^a, Wonsuk Chung^b, Hyejin Lee^c, Seungman Park^d, Jay H. Lee^{b,*}^a Process Systems Engineering (AVT.SVT), RWTH Aachen University, Forckenbeckstraße 51, 52074 Aachen, Germany^b Department of Chemical and Biomolecular Engineering, Korea Advanced Institute of Science and Technology (KAIST), 291 Daehak-ro, Yuseong-gu, Daejeon 34141, Republic of Korea^c Department of Agricultural & Resource Economics, Seoul National University, 1 Gwanak-ro, Gwanak-Gu, Seoul 08826, Republic of Korea^d Enertopia Korea, 511 Yeongdong-Daero, Gangnam-Gu, Seoul 06164, Republic of Korea

ARTICLE INFO

Article history:

Received 31 December 2019

Received in revised form 18 March 2020

Accepted 23 March 2020

Available online xxxx

Keywords:

Power-to-Gas

Co-electrolysis

CO₂ capture and utilization

TIMES

Excess electricity

Syngas

ABSTRACT

This work analyzes the impacts of deploying a Power-to-Gas technology in the power generation sector in South Korea by 2050. The Power-to-Gas technology of interest is the low-temperature co-electrolysis of CO₂ and H₂O, which is an emerging technology for electrochemically converting them to syngas. Particularly, excess electricity available from intermittent renewable energy resources is intended to be the main energy source for the co-electrolysis. A conceptual design of the co-electrolysis process is carried out to calculate its performance data including mass balances, energy demand, and capital investment. Based on them, a temporal energy system model is developed using the TIMES (The Integrated MARKAL-EFOM System) model generator. The conclusion is that deploying the co-electrolysis process in the Korean power generation sector can reduce greenhouse gas emissions and also save the overall system cost when the syngas production cost is lower than the purchasing cost of liquid natural gas. The beneficial impacts are limited by the amount of available excess electricity and the co-firing ratio limit in the gas-fired power plants. Finally, the overpotential and current density, as uncertain parameters of the co-electrolysis process, are found to affect the syngas production cost most strongly.

© 2020 The Authors. Published by Elsevier Ltd. This is an open access article under the CC BY-NC-ND license (<http://creativecommons.org/licenses/by-nc-nd/4.0/>).

1. Introduction

Use of renewable energy resources in power generation has recently been accelerated due to the rising concern about climate change. In 2017, renewables-based electricity generation increased by 6.3% (380 TWh) to account for 25% of global electricity generation. In particular, wind power and solar photovoltaic (PV) grew at the pace of 36% and 27%, respectively (OECD/IEA, 2018). However, the availability of such resources is inherently intermittent so that their power generation rates highly fluctuate. As a result, their continued penetration into the power sector will lead to a grid instability problem caused by supply–demand imbalance. To solve this problem, excess electricity occurring during high generation periods should be stored for later use. Batteries are the best known solutions to this and lithium-ion batteries in particular are best positioned to meet the requirement for electric energy storage in the near future given its high round-trip efficiency (70%–80%) (Schimpe et al., 2018). However, the energy density of batteries is not high and its cost is not cheap enough

for long-term energy storage on a large scale (Blanco and Faaij, 2018).

Power-to-X (P2X) is an alternative to batteries for electric energy storage. Herein, various applications come into X such as heat (Power-to-Heat), gas fuel (Power-to-Gas), liquid fuel (Power-to-Liquid), and chemical compounds (Power-to-Chemical) (Burre et al., 2020). P2X technology can store excess electricity arising from renewable power as chemical bonds in gases or liquids, which have the advantage of high energy density. Thus, it suits the purpose of long-term electricity storage (Blanco and Faaij, 2018). For example, we can utilize carbon dioxide (CO₂) as backbones in synthesis of various organic compounds such as carbon monoxide (CO), acids, alcohols, and hydrocarbons (Jouny et al., 2018), which are mostly produced with fossil based feedstocks today. Thus, it has the potential to mitigate greenhouse gas (GHG) emissions. Moreover, countries lacking fossil fuel or small islands can improve their energy security by producing fuels domestically (Ölz et al., 2007). Finally, energy stored in such forms can be transported by pre-existing infrastructure and vehicles without extensive modifications and substantial capital investment.

As a promising P2X technology low-temperature (LT) co-electrolysis of CO₂ and water (H₂O) recently has attracted much

* Corresponding author.

E-mail address: jayhlee@kaist.ac.kr (J.H. Lee).

attention from both academia and even industry (Sánchez et al., 2019). LT co-electrolysis can produce syngas, a mixture of H₂ and CO, at a ratio controlled by suitable choices of catalyst, reactor design, and operation (Sheng et al., 2017). For example, the H₂/CO ratio of ~2 fits the synthesis of methanol (Olah et al., 2009) and liquid hydrocarbon (Dry, 2002), whereas the ratio of 1 is suitable for the synthesis of dimethyl ether (DME) (Schakel et al., 2016) and acetic acid (Roh et al., 2018). Also, the produced syngas can be combusted at gas-fired power plants as a supplementary fuel. Compared to other two-step Power-to-Gas pathways such as *water electrolysis & reverse water gas shift (RWGS)* and *water electrolysis & CO₂ methanation*, the LT co-electrolysis has a simpler system configuration as it requires a one-step processing (i.e., electrolysis) for syngas production (Vennekötter et al., 2019b). Also, we can start-up alkaline or proton exchange membrane (PEM) electrolyzers more quickly than another alternative high-temperature co-electrolysis (also known as solid oxide electrolyzer cell) (Buttler and Spliethoff, 2018). Therefore, the LT co-electrolysis process would be suitable for adjusting the operation to the fluctuation in electricity spot prices and/or availability or offering the capacity to a power grid upon request from a transmission system operator (TSO) for the grid balancing. However, there is a need for the development of low-cost (i.e., earth-abundant based), efficient, and selective catalysts which can replace the current noble metal-based catalysts such as silver, gold, and platinum (Hernández et al., 2017). Achieving high current density with low overpotential (Möller et al., 2019) and mitigating the product crossover (Lin et al., 2019) are other challenges that should be overcome. Also, we should investigate the electrolysis cell design process and electrode configuration, which influence the operation stability, energetic efficient transformation, and product spectrum (Vennekötter et al., 2019b).

No one has yet assessed the LT co-electrolysis technology for the purpose of producing syngas as a fuel for power generation. Li et al. (2016) and Spurgeon and Kumar (2018) analyzed the economic potential and GHG emissions of the co-electrolysis technology for syngas production, which is subsequently converted into *liquid fuel* through the Fischer–Tropsch Process. Most of other previous studies for LT co-electrolysis technology assessment are limited to chemical production (Agarwal et al., 2011; Jouny et al., 2018; Na et al., 2019; Verma et al., 2016). Furthermore, beyond the standalone analysis, we should analyze how the technology affects existing systems such as energy systems, industries, residential area, and transportation when it is implemented. By definition, P2X is intended to use excess electricity arising from renewable power. Also, if the technology is to produce another form of energy resource, it has to compete with conventional energy resources in terms of costs. Therefore, it is essential to analyze the LT co-electrolysis technology in association with the power generation sector such as the work of Blanco et al. (2018) and Lee (2019).

We analyze the impacts of deploying the LT co-electrolysis technology in the power generation sector in terms of economics and GHG reduction. As a case study, we assume that the LT co-electrolysis technology is commercially introduced to the power generation sector in South Korea from year 2030 and gradually deployed until 2050. CO₂ captured from gas-fired power plants are to be used as the feedstock. The produced syngas is subsequently mixed with natural gas and supplied to the gas-fired power plant to close the carbon cycle. A conceptual design of the syngas production process employing the co-electrolysis is carried out to calculate mass balance, energy demand, and capital investment. Then, a temporal energy system model of Korea from 2020 to 2050 is developed using the TIMES (The Integrated MARKAL-EFOM System (Loulou et al., 2005)) model generator

given the national statistics and outlook data. The model can be used to estimate when and how much excess electricity will be available. Based on the information, the calculation is carried out for how much syngas can be produced via the co-electrolysis and how the GHG emissions and system costs of the power generation sector are influenced. Moreover, key performance parameters of the co-electrolysis process are perturbed to see how significant their influences are on the analysis results.

2. Description of the co-electrolysis process

The analyzed systems for the co-electrolysis comprises three sections: the power generation, the CO₂ capture, and the co-electrolysis of CO₂ and H₂O (Fig. 1). In the power generation section (R2), we assume a gas turbine combined cycle (GTCC) power plant that utilizes fuel gas such as methane and syngas. The fuel combustion yields flue gas containing CO₂ in 3~5 mol.%. In the CO₂ capture section (S2), an absorption process using a novel polyamine solvent called MAB (Modulated Amine Blend) is used to capture the CO₂ present in the flue gas. MAB has been reported to outperform the conventional monoethanolamine (MEA) solvent in terms of solvent regeneration energy as well as cost of CO₂ avoided (Yun et al., 2018). The low-pressure (LP) steam needed for regenerating the MAB solvent is assumed to be purchased from outside. The captured CO₂ is compressed up to 20 bar via 2-stage compressors and sent to PEM electrolyzer cells (R1). Only the excess electricity is assumed to be used in this process. Deionized process water is supplied to the cells along with CO₂. Syngas and oxygen (O₂) are produced at the cathode and anode sides, respectively. Most of the unreacted CO₂ and H₂O in R1 are recovered (S1) and recycled. The produced syngas is assumed to be sent back to R2 as the main fuel. Since not all of the CO₂ in the flue gas is captured, natural gas is supplemented to close the carbon balance.

3. Process simulation and analysis

The overall analysis follows the evaluation procedure for emerging CO₂ utilization technologies, proposed by Roh et al. (2019). Process simulation and analysis require a set of input data such as process design specifications, prices, and carbon emission factors. The co-electrolysis technology is currently at TRL3 and is assumed to be available for commercial deployment starting year 2030. Thus, we assume improved performance and economic parameters, e.g., cell overpotential, current density, and purchasing cost of the electrolyzer cells, compared to the current state-of-the-art technologies at a lab-scale (Vennekötter et al., 2019a,b). The achievable values of such performance parameters in the future are highly uncertain, so three different values are assumed each for the parameters. Other design specifications and assumptions are as follows:

- GTCC power plants internally supply electricity to the compressors for stable operation.
- The energy efficiency of GTCC power plants is constant at 49%, regardless of the co-firing ratio.
- O₂ byproduct post-treatments such as dehumidification and pressurization are not considered.
- Low pressure (LP) steam for the solvent regeneration is produced at liquid natural gas (LNG) boilers.
- Electric energy demand for the CO₂ capture is excluded because it is negligible (Yun et al., 2018).
- The open-circuit potential is 1.281 V, estimated from the standard Gibbs energy. The actual potential is the sum of the open-circuit potential and the cell overpotential.
- No side-product from the co-electrolysis is generated.

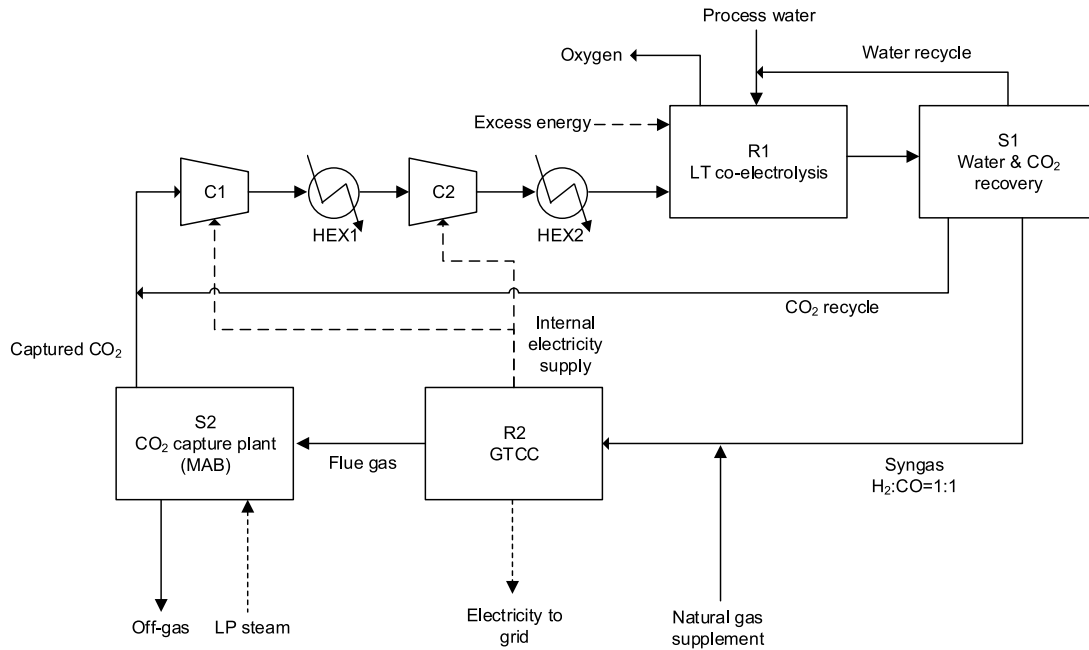


Fig. 1. Block flow diagram of the co-electrolysis process integrated with the GTCC power plant and the MAB-based CO₂ capture plant.

- Unreacted CO₂ is recovered by pressure swing adsorption (PSA).
- Water and CO₂ are recovered with 100% purity.
- Capital investments for the water and CO₂ recovery units and intercoolers are excluded since they are far lower than those for the electrolyzer cells and compressors.

All the primary data assumed in this study are given in Table 1.

Given the primary data, secondary data including mass balances and energy demands are calculated using the commercial simulator of Aspen Plus[®]. The calculation results are shown in Table 2. It should be noted that the electric power consumption for the co-electrolysis largely dominates the other energy consumptions in all the scenarios.

Based on the calculated secondary data, capital costs of the process are estimated. Total capital investment is calculated by multiplying appropriate factors with total installed cost (TIC). Fig. 2 represents that the PEM electrolyzer cell accounts for the largest portion of TIC in all the scenarios followed by the compressors. Because of the large flow rate of the recycled CO₂, the TIC of the compressors exceeds that of the CO₂ capture unit. The multiplication factors and the calculated capital and fixed costs (i.e. operation & maintenance costs) are given in Table S1 and Table S2 in the Supplementary Material (SM), respectively.

4. Analyzing the impacts of deploying the co-electrolysis processes on the power generation sector in South Korea

4.1. TIMES model description

We develop a temporal energy systems model that mimics the power generation sector in South Korea by using the TIMES model generator (IEA-ETSAP, 2019). As the model is data-driven, we need a large amount of input data such as the performance data of 21 different types of power plants, plans for construction and deconstruction of the power plants, forecasts for electricity demand and resource prices, and so on. Solving a linear program in GAMS (General Algebraic Modeling System), we obtain long-term policies such as energy systems configuration, energy flows, energy commodity prices, GHG emissions, capacities of technologies, energy costs, and marginal emissions abatement costs, while

meeting the given constraints (e.g. electricity demand and target GHG reduction) at minimum system cost (IEA-ETSAP, 2019).

The basic model structure is referred from Lee (2019). We assume that the electricity supply is allowed to be greater than the electricity demand. The inequality in the place of the usual equality allows for excess electricity generation given the intermittency of the solar PV and wind power. 16 time slices (see Table S10 in the SM) are used to represent one year time horizon.

The annual excess electricity (Lee, 2019) is calculated by

$$\begin{aligned} \text{Excess Electricity}(t) &= \text{Power Generation}(t) \\ &\quad - \text{Pumped Storage Usage}(t) \\ &\quad - \text{Transmission and Distribution Loss}(t) - \text{Electricity Demand}(t) \end{aligned}$$

$$\text{Annual Excess Electricity}(y) = \sum_t \text{Excess Electricity}(t)$$

where t and y indicate time slices and years. The annual system costs are calculated by

$$\text{System Cost}(y) = \text{Power Plant Variable Cost}(y)$$

$$+ \text{Power Plant Fixed Cost}(y)$$

$$+ \text{Power Plant Investment Cost}(y) + \text{Fuel Cost}(y)$$

$$\text{Power Plant Variable Cost}(y) = \sum_e \{ \text{Power Generation}(y, e) \times \text{Variable Cost}(y, e) \}$$

$$\text{Power Plant Fixed Cost}(y) = \sum_e \{ \text{Power Plant Capacity}(y, e) \times \text{Fixed Cost}(y, e) \}$$

$$\text{Power Plant Investment Cost}(y)$$

$$= \sum_e \{ \text{Power Plant New Capacity}(y, e) \times \text{Investment Cost}(y, e) \}$$

$$\text{Fuel Cost}(y) = \sum_f \{ \text{Fuel Use}(y, f) \times \text{Fuel Price}(y, f) \}$$

where e and f indicate power generation facilities and fuels, respectively. Annual GHG emissions are calculated by

$$\text{GHG Emissions}(y) = \sum_f \{ \text{Fuel Use}(y, f) \times \text{Emissions Factor}(f) \}$$

Other assumptions used in developing the TIMES model and input data such as Annual Electricity Demand, Emissions Factor and Fuel Price are described in Section 2 in the SM.

Fig. 3 illustrates the reference energy systems represented by the TIMES model. Syngas production is associated with the GTCC

Table 1
Primary data of the co-electrolysis process.

| Specification | Unit | Value | Note |
|---|-----------------------|---------------------|--|
| Co-electrolysis section | | | |
| Pressure | Bar | 20 | Typical operating range of a PEM electrolyzer (Carmo et al., 2013) |
| Temperature | °C | 40 | |
| Cell overpotential | V | 0.5, 1, 1.5 | Own assumption. Around 2V of cell overpotential was measured at recent lab-scale experiments (Vennekötter et al., 2019a) |
| Current density | mA/cm ² | 200, 350, 500 | Own assumption. 150mA/cm ² was achieved by recent lab-scale experiments (Vennekötter et al., 2019a) |
| Faradaic efficiency | % | | |
| H ₂ | | 50 | Experimental results (Vennekötter et al., 2019a) |
| CO | | 50 | |
| Per-pass CO ₂ conversion rate | % | 30 | Experimental results (Dufek et al., 2011) |
| CO ₂ recovery rate from the syngas | % | 90 | Own assumption |
| PEM electrolyzer cell purchasing cost | USD/m ² | 1,840, 2,760, 3,680 | Own assumption. 1,840 USD/m ² was assumed by Jouny et al. (2018) for alkaline electrolyzers. IEA (2015) reported that PEM electrolyzers are twice as expensive as alkaline electrolyzers. |
| Power generation section | | | |
| Net power generation | GW | 1 | |
| GTCC efficiency | % | 49 | |
| CO₂ capture section | | | |
| CO ₂ capture rate | % | 90 | Own assumption |
| MAB solvent regeneration energy | GJ/ton _{CO2} | 2.81 | Simulation results (Yun et al., 2018) |
| Compressor efficiency | % | 80 | |

Table 2
Secondary data of the co-electrolysis process – Mass balance and energy demand.

| Specification | Unit | Value |
|--|--|--|
| Mass balance | | |
| Product | | |
| Syngas production rate (Heat flow rate – LHV basis) | ton/GJ _{EI} (GJ/GJ _{EI}) | 0.149 (1.939) |
| Oxygen production rate | ton/GJ _{EI} | 0.118 |
| CO ₂ | | |
| Captured CO ₂ flow rate | ton/GJ _{EI} | 0.201 |
| Recycled CO ₂ flow rate | ton/GJ _{EI} | 0.341 |
| Emitted CO ₂ flow rate | ton/GJ _{EI} | 0.022 |
| Process water feed rate | ton/GJ _{EI} | 0.067 |
| Thermal energy demand | | |
| Steam demand for CO ₂ capture | GJ/GJ _{EI} | 0.563 |
| Natural gas supplement (LHV basis) | GJ/GJ _{EI} | 0.396 |
| Electric energy demand | | |
| Power demand for co-electrolysis | GJ/GJ _{EI} | (0.5V) 2.540 (1.0V) 2.896 (1.5V) 3.253 |
| CO ₂ compression | GJ/GJ _{EI} | 0.144 |
| Other energy demand | | |
| Cooling water | GJ/GJ _{EI} | 0.154 |

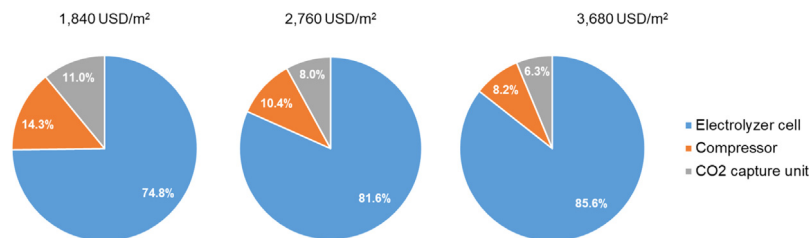


Fig. 2. Breakdown of the TIC for three different PEM electrolyzer cell prices. Current density of the base case (350 mA/cm²) is assumed.

power plants. Capturing CO₂ in the flue gas emitted from the GTCC power plants, we produce the syngas via the co-electrolysis

and supply it to the GTCC power plant as the feed. In South Korea there is no electricity balancing market for grid stabilization

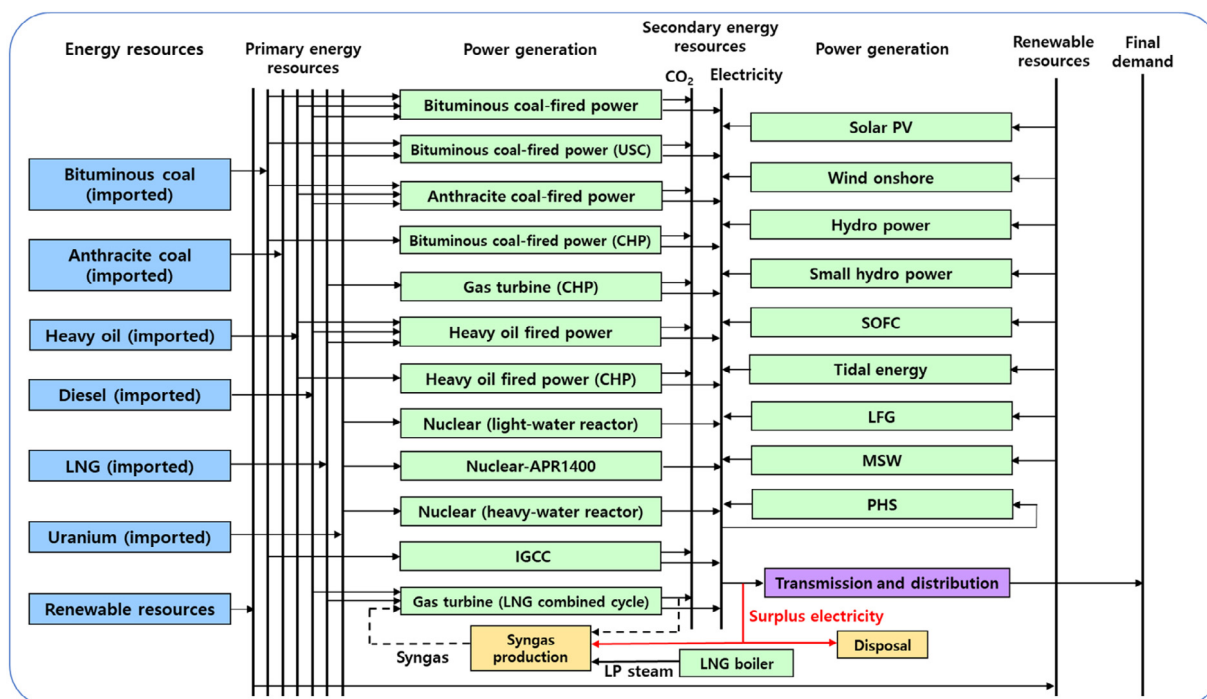


Fig. 3. Illustration of the Korean energy systems adopted by the TIMES model developed.

and the excess electricity is disposed, so we assume that excess electricity is either consumed by the co-electrolysis process without any cost or simply disposed when the syngas production is economically not competitive to importing LNG. The LNG boiler is used to supply the LP steam for regenerating the MAB solvent in the CO₂ capture.

4.2. Scenario description

Table 3 represents five key parameters of the co-electrolysis process in three different cases. The values of the cell overpotential, current density and the capital investment for the electrolyzer cells are the same as in Section 2. The maximum allowable co-firing ratio of the syngas to the typical imported natural gas (Kyungdong City Gas, 2019) is 2.1%, which complies with the minimum CH₄ content limit (85 mol.%, Choi (2004)) of natural gas transported via pipeline in South Korea. Twice and one half of the value for the co-firing ratio in the base case are assumed for the high and low performance cases, respectively. The annual availability of the co-electrolysis process for the high performance case (95%) is taken from Lee (2019), and we reduced it by 5% and 10% for the base and low performance cases, respectively.

We generate 14 scenarios as listed in Table 4. Scenario 1 is the baseline scenario that allows for deploying the co-electrolysis process. Scenario 2 to 11 are intended to investigate sensitivity of the five key parameters of the co-electrolysis process. Scenario 12 and 13 are two extreme cases. Finally, Scenario 14 is the reference scenario that does not allow for deploying the co-electrolysis process.

4.3. Analysis results

4.3.1. Reference scenario

For the reference scenario where the syngas production via the co-electrolysis is not considered, the power capacity and electricity generation of each power source from 2020 to 2050 are calculated using the TIMES model we developed. Here, we by the TIMES model developed power capacity and generation

of electricity where the co-electrolysis-based syngas production plant is not considered. In order to meet the electricity demand forecasted (see Figure S1 in the SM), the total power capacity and total electricity generation increase by 58.6% and 11.9%, respectively, from year 2020 to 2050, as shown in Fig. 4. The portions of solar PV and wind power in the capacity as well as in the actual power generation greatly increase while those of nuclear, coal-fired, and gas-fired power plants gradually decrease. In particular, the solar PV accounts for the biggest portion of the total power capacity from year 2032. Nevertheless, it does not supply the largest amount of electricity due to its low annual availability (15%). GTCC power plants are often operated at part loads as their major role is to meet the peak demand. Thus, their contribution to the power generation is not as big as to the power capacity. In contrast, the coal-fired and nuclear power plants are responsible for the base load, so they keep high utilization rates. Because of the large amount of renewable power introduced to the energy systems, the overall GHG emissions are gradually decreasing over the years (Fig. 5).

4.3.2. Excess electricity

Excess electricity originates from the discrepancy between electricity generation and demand. Such a gap especially arises due to intermittent solar and wind energy. In the TIMES model, we impose an inequality constraint instead of the usual equality constraint, which allowed the total electricity generation to surpass the total electricity demand. As shown in Fig. 6, the year of 2039 is the first moment when the excess electricity is generated. Until then, no excess electricity is found as the total electricity demand is met by flexible operation of the conventional power sources such as coal-fired and gas-fired power plants and hydropower. As time goes by, more excess electricity is generated due to the increased capacities of solar PV and wind power in the power generation sector. The excess electricity accounts for as high as 1.27% of the total electricity production in 2050.

Table 3

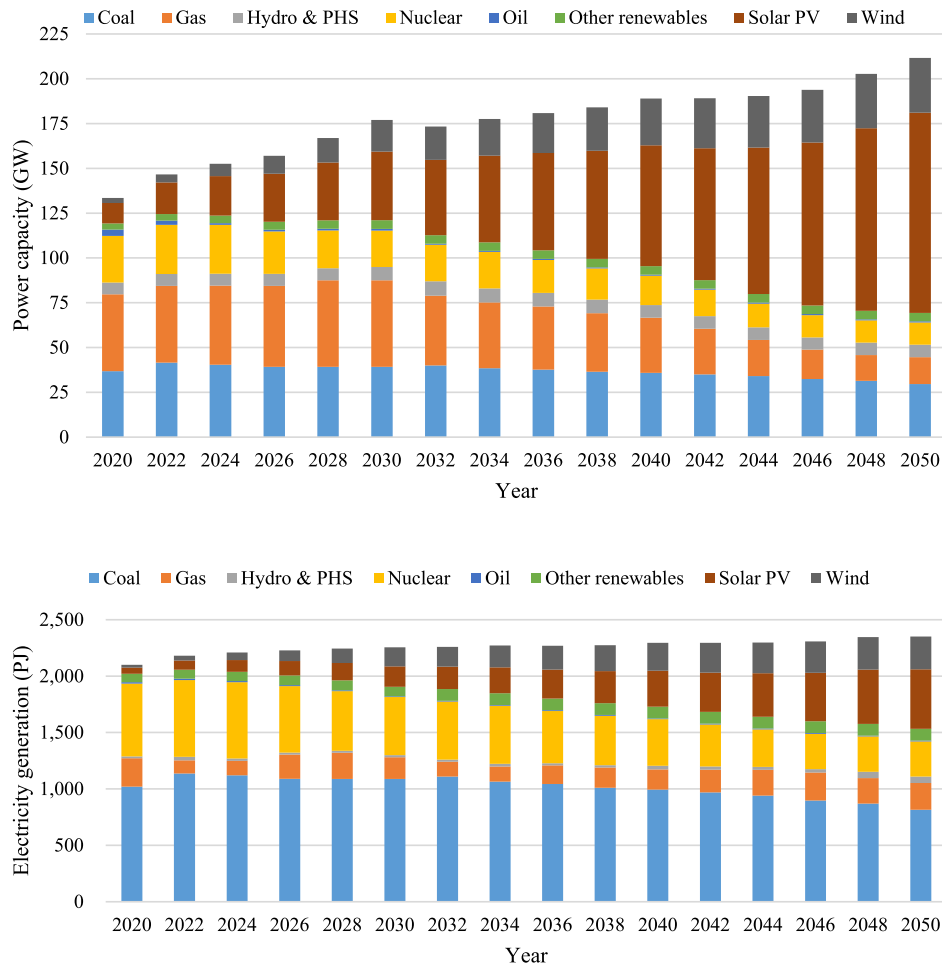
Five key parameters of the co-electrolysis process and their values in three different cases.

| | Unit | High performance | Base case | Low performance |
|---|--------------------|------------------|-----------|-----------------|
| Cell overpotential | V | 0.5 | 1.0 | 1.5 |
| Current density | mA/cm ² | 500 | 350 | 200 |
| Capital investment for electrolyzer cells | USD/m ² | 1,840 | 2,760 | 3,680 |
| Co-firing ratio (heating value basis) | % | 4 | 2.1 | 1 |
| Annual availability | % | 95 | 90 | 85 |

Table 4

The list of scenarios. B indicates the base case, H the high performance case, and L the low performance case in Table 3.

| Scenario # | Cell overpotential | Current density | Capital investment for electrolyzer cells | Co-firing ratio | Annual availability | Note |
|------------|--------------------|-----------------|---|-----------------|---------------------|---|
| 1 | B | B | B | B | B | Baseline scenario |
| 2 | H | B | B | B | B | Cell overpotential sensitivity |
| 3 | L | B | B | B | B | Cell overpotential sensitivity |
| 4 | B | H | B | B | B | Current density sensitivity |
| 5 | B | L | B | B | B | Current density sensitivity |
| 6 | B | B | H | B | B | Cell purchasing cost sensitivity |
| 7 | B | B | L | B | B | Cell purchasing cost sensitivity |
| 8 | B | B | B | H | B | Co-firing ratio sensitivity |
| 9 | B | B | B | L | B | Co-firing ratio sensitivity |
| 10 | B | B | B | B | H | Annual availability sensitivity |
| 11 | B | B | B | B | L | Annual availability sensitivity |
| 12 | H | H | H | H | H | Most optimistic scenario |
| 13 | L | L | L | L | L | Most pessimistic scenario |
| 14 | N/A | N/A | N/A | N/A | N/A | Reference scenario (No syngas production) |

**Fig. 4.** Distributions of the power generation capacity (top) and electricity production (bottom) from 2020 to 2050 calculated by the TIMES model. Excess electricity generation is allowed while no syngas production is considered.

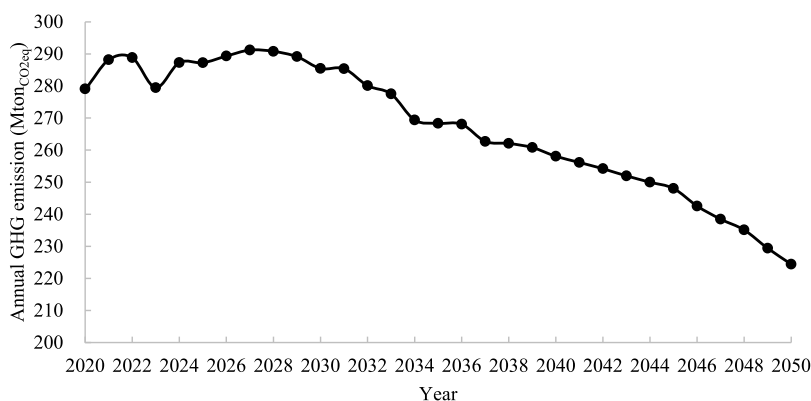


Fig. 5. GHG emissions from the power generation sector in South Korea from 2020 to 2050 in the reference scenario. Excess electricity generation is allowed while no syngas production is considered. A drop in GHG emissions in 2023 is due to the decrease in the power generation from coal-fired power plants. In 2024, the emissions are increased due to the decrease in the nuclear power capacity, which is compensated by the coal-fired power plants.

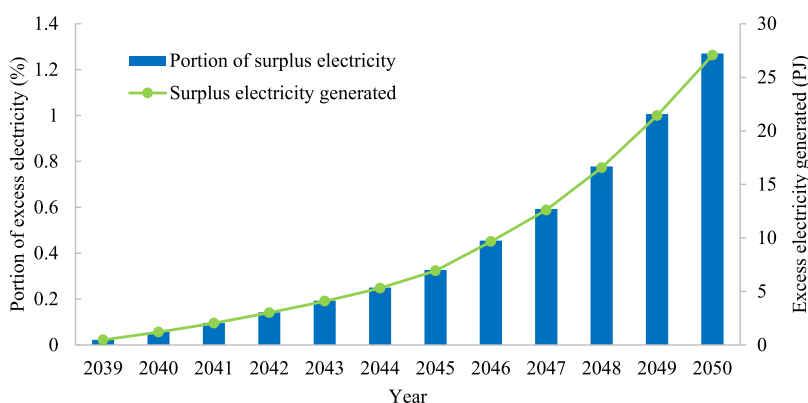


Fig. 6. The amount of excess electricity generated and its portion out of the total electricity production calculated by the TIMES model. No excess electricity is generated before 2039.

4.3.3. Introducing syngas production via the co-electrolysis

When the excess electricity is available and the syngas production is cheaper than purchasing the LNG, the syngas is produced by the co-electrolysis. In the baseline scenario, the amount of the syngas produced and the LNG replaced are increased over the year, as shown in Fig. 7. Also, the increase in the available excess electricity results in the increase in the syngas production. As a result, 2.1% of the total LNG is replaced by the syngas in 2050. As shown in Fig. 8, the co-electrolysis process fully utilizes the available excess electricity until 2046. After that, the utilization rate is decreased as the co-firing ratio (2.1%) constraint comes into effect. Thus, the syngas production remains the same from 2047 to 2048. Only 53.2% of the available excess electricity is consumed by the co-electrolysis in 2050. Note that the deployment of the co-electrolysis process does not significantly change the composition of the entire power system as the amount of excess electricity available is small compared to the total electricity generated.

Table 5 represents how the key parameters of the co-electrolysis process affect the utilization rate of the excess electricity. More excess electricity is consumed by the co-electrolysis process in Scenario 2 than in Scenario 1. In Scenario 2, due to the lower cell overpotential, less electricity is needed for the syngas production than in Scenario 1. The opposite trend appears in Scenario 3. In Scenario 5, due to the low current density, the total cost for purchasing the electrolyzer cells makes the syngas production cost higher than the LNG purchase price. Therefore,

the syngas is never produced in spite of the free excess electricity. In Scenario 8 and 9, the changes in the co-firing ratio, a key limiting factor, significantly affect the utilization rate of the excess electricity. In Scenario 8, the excess electricity is always fully utilized whereas in Scenario 9 only 25.3% of the excess electricity is consumed in 2050. In Scenario 4, 6, 7, 10 and 11, the amount of the syngas produced is not affected by the perturbed parameters as they are not the limiting factors, so the utilization rates are the same as in Scenario 1. Less excess electricity is consumed in Scenario 12, the most optimistic scenario, than in Scenario 8. However, more syngas is produced (18.4 PJ in 2050) in that scenario than in Scenario 6 (18.1 PJ in 2050) due to the lower cell overpotential in the former. In Scenario 13, the most pessimistic scenario, no syngas is produced so that the utilization rates are zero during the whole period.

4.3.4. GHG reduction and system cost saving

GHG emissions in the power generation sector are mitigated by deploying the co-electrolysis processes, as depicted in Fig. 9. 0.91 and 0.48 MtonCO_{2eq} could potentially be reduced in year 2050 in the baseline (Scenario 1) and optimistic (Scenario 12) scenarios, respectively. Such reductions are equivalent to 0.40% and 0.21% reduction in the GHG emissions with respect to the reference scenario.

The overall power system cost is reduced as the syngas production replaces the purchase of LNG for GTCC power plants. As shown in Fig. 10, the savings in the system cost per ton of CO₂-equivalent avoided in both the optimistic and baseline scenarios

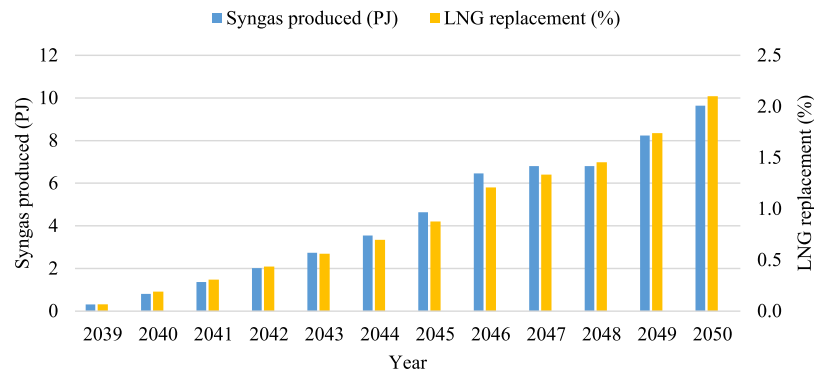


Fig. 7. The amount of syngas produced and the percentage of LNG replacement for gas-fired power generation from 2039 to 2050 in Scenario 1.

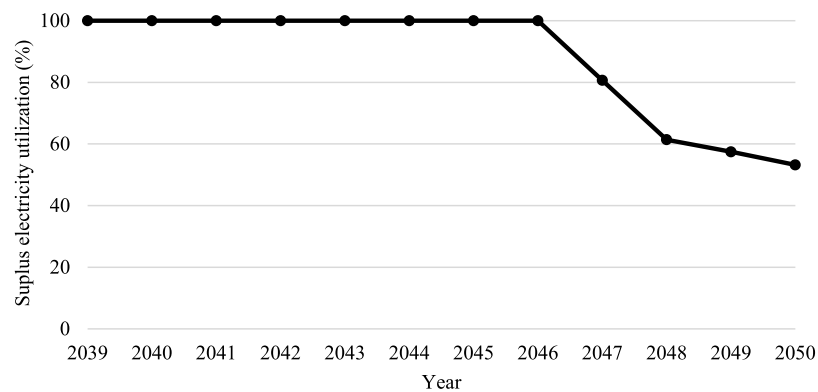


Fig. 8. Utilization rate of the excess electricity from 2039 to 2050 in Scenario 1. 100% indicates all the excess electricity is used for the syngas production while 0% means it is completely disposed.

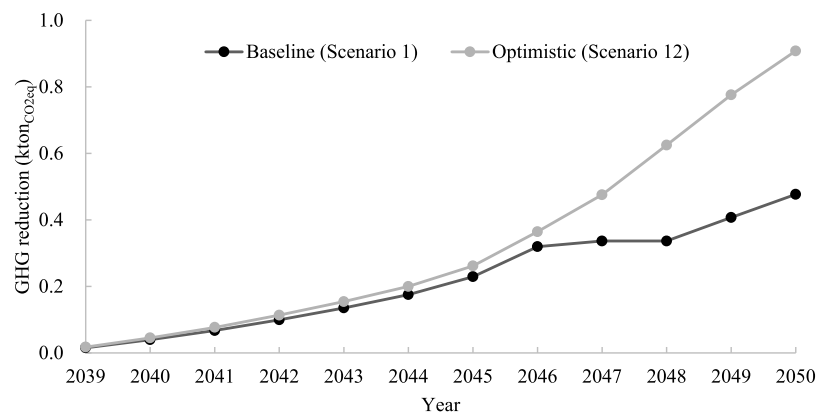


Fig. 9. Reduction in GHG emissions by deploying the co-electrolysis processes from 2039 to 2050 in Scenario 1 (baseline) and 12 (optimistic).

are slightly increasing over the years. Such increases arise from the trend of the LNG price, which is assumed to increase over the time horizon (see Table S5 in the SM). Compared to Scenario 1, 190% higher saving is expected for Scenario 12 due to the lower syngas production cost. Note that the performance (e.g., power demand) and economic parameters (e.g., capital investment) of the syngas production are assumed to be constant in this study, so it results in the constant syngas production cost.

GHG reduction and system cost savings for all the scenarios are given in Table S11 and S12 in Section 3 of the SM, respectively.

5. Conclusion

The impacts of deploying the co-electrolysis of CO₂ and H₂O utilizing excess electricity in the power generation sector in South Korea are investigated. In the studied scenario, syngas is produced via the low-temperature co-electrolysis for power generation at gas-fired combined cycle power plants. To this end, a conceptual design of the co-electrolysis process is carried out to obtain the key input data required for the temporal national energy systems model (i.e., the TIMES model). Then the model is used to simulate the power generation sector for next 30 years (2020~2050). We found that deploying the co-electrolysis process could reduce the national greenhouse gas emissions while saving the system costs by replacing liquid natural gas purchase for gas-fired combined

Table 5

Utilization rates of excess electricity for the syngas production via the co-electrolysis. 100% indicates all the excess electricity is used for the syngas production while 0% does it is completely disposed.

| Scenario # | 2039 | 2040 | 2041 | 2042 | 2043 | 2044 | 2045 | 2046 | 2047 | 2048 | 2049 | 2050 |
|------------|-------|-------|-------|-------|-------|-------|-------|-------|-------|-------|-------|-------|
| 1 | 100.0 | 100.0 | 100.0 | 100.0 | 100.0 | 100.0 | 100.0 | 100.0 | 80.7 | 61.4 | 57.5 | 53.2 |
| 2 | 100.0 | 100.0 | 100.0 | 100.0 | 100.0 | 100.0 | 100.0 | 92.3 | 70.7 | 53.8 | 50.4 | 46.7 |
| 3 | 100.0 | 100.0 | 100.0 | 100.0 | 100.0 | 100.0 | 100.0 | 100.0 | 90.6 | 69.0 | 64.5 | 59.8 |
| 4 | 100.0 | 100.0 | 100.0 | 100.0 | 100.0 | 100.0 | 100.0 | 100.0 | 80.7 | 61.4 | 57.5 | 53.2 |
| 5 | 0.0 | 0.0 | 0.0 | 0.0 | 0.0 | 0.0 | 0.0 | 0.0 | 0.0 | 0.0 | 0.0 | 0.0 |
| 6 | 100.0 | 100.0 | 100.0 | 100.0 | 100.0 | 100.0 | 100.0 | 100.0 | 80.7 | 61.4 | 57.5 | 53.2 |
| 7 | 100.0 | 100.0 | 100.0 | 100.0 | 100.0 | 100.0 | 100.0 | 100.0 | 80.7 | 61.4 | 57.5 | 53.2 |
| 8 | 100.0 | 100.0 | 100.0 | 100.0 | 100.0 | 100.0 | 100.0 | 100.0 | 100.0 | 100.0 | 100.0 | 100.0 |
| 9 | 100.0 | 100.0 | 100.0 | 100.0 | 100.0 | 100.0 | 87.1 | 68.3 | 50.1 | 38.4 | 29.2 | 25.3 |
| 10 | 100.0 | 100.0 | 100.0 | 100.0 | 100.0 | 100.0 | 100.0 | 100.0 | 80.7 | 61.4 | 57.5 | 53.2 |
| 11 | 100.0 | 100.0 | 100.0 | 100.0 | 100.0 | 100.0 | 100.0 | 100.0 | 80.7 | 61.4 | 57.5 | 53.2 |
| 12 | 100.0 | 100.0 | 100.0 | 100.0 | 100.0 | 100.0 | 100.0 | 100.0 | 100.0 | 100.0 | 96.0 | 88.9 |
| 13 | 0.0 | 0.0 | 0.0 | 0.0 | 0.0 | 0.0 | 0.0 | 0.0 | 0.0 | 0.0 | 0.0 | 0.0 |

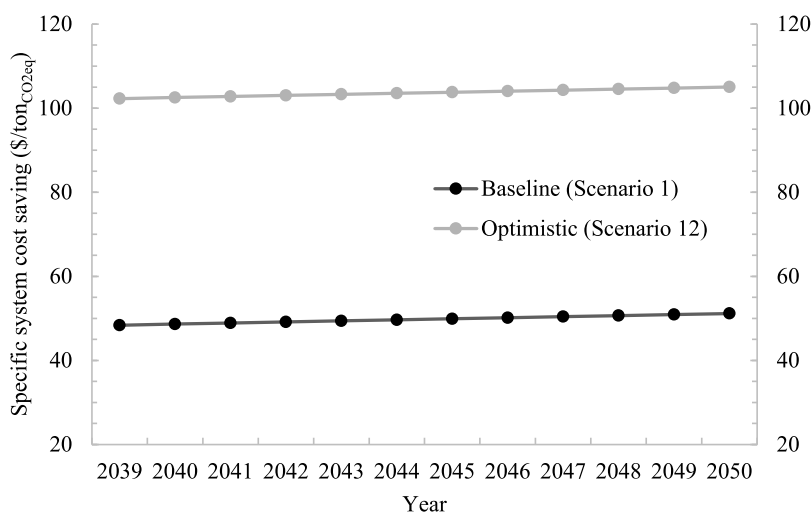


Fig. 10. Savings in the entire power system cost due to deploying the co-electrolysis process from 2039 to 2050 in Scenario 1 (baseline) and 12 (optimistic).

cycle power plants. Among the uncertain parameters of the co-electrolysis, the cell overpotential and current density affect the syngas production cost and the produced amount most significantly. In addition, the co-firing ratio constraint and the amount of excess electricity available acted as the limiting factors.

Several issues remain to be tackled. Uncertainty arising from the renewable power generation needs to be addressed in the analysis. *KPX (2018)* reported that the estimation of the electricity generated by solar photovoltaic and wind power differs from the measurement by 5~15% and 8.4~19%, respectively. Therefore, the potential impacts of the co-electrolysis process on the energy system could be bigger as more excess electricity would be available than we calculated. Moreover, it should be investigated whether the co-firing with syngas at gas-fired combined cycle power plants results in different power generation efficiencies and reflect the difference in the analysis. Also, O₂ by-product resulting from the co-electrolysis should be considered in the TIMES model for more accurate analysis. A main challenge is the lack of reliable data on manufacturing, supply, and demand of O₂ in South Korea. Finally, other Power-to-X technologies such as Power-to-Methane or Power-to-H₂ should be introduced to the TIMES model so that they compete with one another for excess electricity available.

Declaration of competing interest

The authors declare that they have no known competing financial interests or personal relationships that could have appeared to influence the work reported in this paper.

CRediT authorship contribution statement

Kosan Roh: Conceptualization, Methodology, Writing - original draft, Visualization. **Wonsuk Chung:** Methodology, Writing - review & editing. **Hyejin Lee:** Conceptualization, Methodology, Resources, Writing - review & editing. **Seungman Park:** Conceptualization, Methodology, Resources, Writing review & editing. **Jay H. Lee:** Writing - review & editing, Supervision, Funding acquisition.

Acknowledgments

The authors gratefully acknowledge funding by Korea Carbon Capture & Sequestration R&D Center (KCRC) under the project # NRF 2015M1A8A1076118. We are also grateful to Prof. Young Gu Park and Matthias Heßelmann for fruitful discussions.

Appendix A. Supplementary data

Supplementary material related to this article can be found online at <https://doi.org/10.1016/j.egy.2020.03.034>.

References

- Agarwal, A.S., Zhai, Y., Hill, D., Sridhar, N., 2011. The electrochemical reduction of carbon dioxide to formate/formic acid: Engineering and economic feasibility. *ChemSusChem* 4, 1301–1310. <http://dx.doi.org/10.1002/cssc.201100220>.
- Blanco, H., Faaij, A., 2018. A review at the role of storage in energy systems with a focus on power to gas and long-term storage. *Renew. Sustain. Energy Rev* 81, 1049–1086. <http://dx.doi.org/10.1016/j.rser.2017.07.062>.

- Blanco, H., Nijs, W., Ruf, J., Faaij, A., 2018. Potential of power-to-methane in the EU energy transition to a low carbon system using cost optimization. *Appl. Energy* 232, 323–340. <http://dx.doi.org/10.1016/j.apenergy.2018.08.027>.
- Burre, J., Bongartz, D., Brée, L., Roh, K., Mitsos, A., 2020. Power-to-X: Between electricity storage, e-production, and demand side management. *Chem. Ing. Tech.* 92, 74–84. <http://dx.doi.org/10.1002/cite.201900102>.
- Buttler, A., Spliethoff, H., 2018. Current status of water electrolysis for energy storage, grid balancing and sector coupling via power-to-gas and power-to-liquids: A review. *Renew. Sustain. Energy Rev.* 82, 2440–2454. <http://dx.doi.org/10.1016/j.rser.2017.09.003>.
- Carmo, M., Fritz, D.L., Mergel, J., Stolten, D., 2013. A comprehensive review on PEM water electrolysis. *Int. J. Hydrogen Energy* 38, 4901–4934. <http://dx.doi.org/10.1016/j.ijhydene.2013.01.151>.
- Choi, I., 2004. Establishment of natural gas composition standards. [WWW Document]. *Today Energy*. URL <http://www.todayenergy.kr/news/articleView.html?idxno=12343>. (Accessed 3 February 2019).
- Dry, M.E., 2002. High quality diesel via the Fischer–Tropsch process - A review. *J. Chem. Technol. Biotechnol.* 77, 43–50. <http://dx.doi.org/10.1002/jctb.527>.
- Dufek, E.J., Lister, T.E., McIlwain, M.E., 2011. Bench-scale electrochemical system for generation of CO and syn-gas. *J. Appl. Electrochem.* 41, 623–631. <http://dx.doi.org/10.1007/s10800-011-0271-6>.
- Hernández, S., Farkhondeh, M.Amin., Sastre, F., Makkee, M., Saracco, G., Russo, N., 2017. Syngas production from electrochemical reduction of CO₂: current status and prospective implementation. *Green Chem.* 19, 2326–2346. <http://dx.doi.org/10.1039/C7GC00398F>.
- IEA, Technology Roadmap: Hydrogen and Fuel Cells. Paris, France.
- IEA-ETSAP, 2019. Overview of TIMES modelling tool. [WWW Document]. URL <https://iea-etsap.org/index.php/etsap-tools/model-generators/times>. (Accessed 10 July 2019).
- Jouny, M., Luc, W., Jiao, F., 2018. General techno-economic analysis of CO₂ electrolysis systems. *Ind. Eng. Chem. Res.* 57, 2165–2177. <http://dx.doi.org/10.1021/acs.iecr.7b03514>.
- KPX, 2018. Advancing the Forecast System of Renewable Power Generation in Jeju. Naju-si, Jeollanam-do, South Korea.
- Kyungdong City Gas, 2019. LNG. [WWW Document]. URL http://mafra.win.korcham.net/nFile/Consult/Business/consult_20140616122122.PDF. (Accessed 4 May 2019).
- Lee, H., 2019. Energy Technologies for Variable Renewable Energy in Power Generation Sector: Focusing on BECCU, Power to Gas Technologies. Ph.D. dissertation. Seoul National University.
- Li, X., Anderson, P., Jhong, H.-R.M., Paster, M., Stubbins, J.F., Kenis, P.J.A., 2016. Greenhouse gas emissions, energy efficiency, and cost of synthetic fuel production using electrochemical CO₂ conversion and the Fischer–Tropsch process. *Energy & Fuels* 30, 5980–5989. <http://dx.doi.org/10.1021/acs.energyfuels.6b00665>.
- Lin, M., Han, L., Singh, M.R., Xiang, C., 2019. An experimental- and simulation-based evaluation of the CO₂ utilization efficiency of aqueous-based electrochemical CO₂ reduction reactors with ion-selective membranes. *ACS Appl. Energy Mater.* 2, 5843–5850. <http://dx.doi.org/10.1021/acs.aem.9b00986>.
- Loulou, R., Remne, U., Kanudia, A., Lehtila, A., Goldsein, G., 2005. Documentation for the TIMES Model. Part I - TIMES Concepts and Theory.
- Möller, T., Ju, W., Bagger, A., Wang, X., Luo, F., Ngo Thanh, T., Varela, A.S., Rossmelsl, J., Strasser, P., 2019. Efficient CO₂ to CO electrolysis on solid Ni–N–C catalysts at industrial current densities. *Energy Environ. Sci.* 12, 640–647. <http://dx.doi.org/10.1039/C8EE02662A>.
- Na, J., Seo, B., Kim, J., Lee, C.W., Lee, H., Hwang, Y.J., Min, B.K., Lee, D.K., Oh, H., Lee, U., 2019. General technoeconomic analysis for electrochemical coproduction coupling carbon dioxide reduction with organic oxidation. *Nat. Commun.* 10, 5193. <http://dx.doi.org/10.1038/s41467-019-12744-y>.
- OECD/IEA, 2018. Global Energy & CO₂ Status Report 2017.
- Olah, G.A., Goeppert, A., Prakash, G.K.S., 2009. Beyond Oil and Gas: The Methanol Economy, second ed. <http://dx.doi.org/10.1002/9783527627806>.
- Ölz, S., Sims, R., Kirchner, N., 2007. Contribution of Renewables to Energy Security. IEA Information Paper.
- Roh, K., Burre, J., Bongartz, D., Lee, S.J.H., Chung, W., Han, D., König, A., Deutz, S., Bardow, A., Lee, J.H., Mitsos, A., 2019. TRL-based guidelines for early-stage evaluation of CO₂ Utilization technologies. In: The 17th International Conference on Carbon Dioxide Utilization (ICCDU 2019), 23 - 27 June 2019, Aachen, Germany.
- Roh, K., Lim, H., Chung, W., Oh, J., Yoo, H., Al-Hunaidy, A.S., Imran, H., Lee, J.H., 2018. Sustainability analysis of CO₂ capture and utilization processes using a computer-aided tool. *J. CO₂ Util.* 26, 60–69. <http://dx.doi.org/10.1016/j.jcou.2018.04.022>.
- Sánchez, O.G., Birdja, Y.Y., Bulut, M., Vaes, J., Breugelmanns, T., Pant, D., 2019. Recent advances in industrial CO₂ electroreduction. *Curr. Opin. Green Sustain. Chem.* 16, 47–56. <http://dx.doi.org/10.1016/j.cogsc.2019.01.005>.
- Schakel, W., Oreggioni, G., Singh, B., Strömman, A., Ramírez, A., 2016. Assessing the techno-environmental performance of CO₂ utilization via dry reforming of methane for the production of dimethyl ether. *J. CO₂ Util.* 16, 138–149. <http://dx.doi.org/10.1016/j.jcou.2016.06.005>.
- Schimpe, M., Naumann, M., Truong, N., Hesse, H.C., Santhanagopalan, S., Saxon, A., Jossen, A., 2018. Energy efficiency evaluation of a stationary lithium-ion battery container storage system via electro-thermal modeling and detailed component analysis. *Appl. Energy* 210, 211–229. <http://dx.doi.org/10.1016/j.apenergy.2017.10.129>.
- Sheng, W., Kattel, S., Yao, S., Yan, B., Liang, Z., Hawxhurst, C.J., Wu, Q., Chen, J.G., 2017. Electrochemical reduction of CO₂ to synthesis gas with controlled CO/H₂ ratios. *Energy Environ. Sci.* 10, 1180–1185. <http://dx.doi.org/10.1039/C7EE00071E>.
- Spurgeon, J.M., Kumar, B., 2018. A comparative technoeconomic analysis of pathways for commercial electrochemical CO₂ reduction to liquid products. *Energy Environ. Sci.* 11, 1536–1551. <http://dx.doi.org/10.1039/C8EE00097B>.
- Vennekötter, J.-B., Scheuermann, T., Sengpiel, R., Wessling, M., 2019a. The electrolyte matters: Stable systems for high rate electrochemical CO₂ reduction. *J. CO₂ Util.* 32, 202–213. <http://dx.doi.org/10.1016/j.jcou.2019.04.007>.
- Vennekötter, J.-B., Sengpiel, R., Wessling, M., 2019b. Beyond the catalyst: How electrode and reactor design determine the product spectrum during electrochemical CO₂ reduction. *Chem. Eng. J.* 364, 89–101. <http://dx.doi.org/10.1016/j.cej.2019.01.045>.
- Verma, S., Kim, B., Jhong, H.-R., Molly, Ma, S., Kenis, P.J.A., 2016. A gross-margin model for defining technoeconomic benchmarks in the electroreduction of CO₂. *ChemSusChem* 9, 1972–1979. <http://dx.doi.org/10.1002/cssc.201600394>.
- Yun, S., Lee, S., Oh, S., Kim, J.-K., 2018. Techno-economic analysis for post-combustion CO₂ capture. In: 8th Korea CCUS International Conference, 24–26 January 2018, Jeju, South Korea.